Modelling the back-to-back power converter for WPGS in the load flow solution by Newton's method

Antônio Baleeiro[1*], Wander G. da Silva[1], Bernardo Alvarenga[1*], Geyverson de Paula[1], Enes Marra[1] and José Nerys[1]

[1]*Escola de Engenharia Elétrica, Mecânica e de Computação, Universidade Federal de Goiás, Brasil*
**Corresponding author. E-mail: baleeiro@ufg.br, bernardo_alvarenga@ufg.br*

ABSTRACT

This paper presents the steady state modelling of a Wind Power Generation System (WPGS) by using the load flow technique. To be connected to the grid, the WPGS demands the use of a power converter in a back-to-back configuration. The load flow technique requires the use of electrical components and nodal analysis where voltages are the unknown variables, referred to as slack, PV and PQ buses. In this work, the back-to-back power converter is modelled as an interface between the WPGS and the AC-60Hz grid. Simulation results are used to validate the model by using the parameters of a fraction of a WPGS plant located in the northeast of Brazil.

Keywords: Newton algorithm; Pulse width modulation; Voltage source converter (VSC).

INTRODUCTION

Renewable electric energy sources such as WPGS demands the use a power converter in the back-to-back array to be connected to the grid [1]. Power systems steady state analysis is usually carried out by using the load flow technique and the modelling is based on nodal analysis where the unknown variables are the voltages on buses type PQ and voltage angles on buses type PV, so that the module and phase angle of voltage in buses referred to as slack are specified [2].

In the load flow analysis, the grid modelling is represented in the frequency domain. The solution of such system is express in terms of node voltages computed from a pre-defined scenario of required active and reactive power from the load's buses, for a given generation level. Among the information obtained about the system's operation in steady state, stand out of calculated nodal voltages in certain buses, besides the losses [2].

In the WPGS, the wind turbine drives a generator which supplies active power to a three-phase active rectifier at variable frequency. The rectifier supplies a capacitor filter with DC voltage (DC link), that feeds a Pulse Width Modulation – PWM inverter which connects the DC link voltage to the 60Hz AC grid. The PWM modulation index, used to control the DC link voltage level, is an unknown variable to be computed together with the node voltages at both ends of the power system. The presence of the back-to-back converter splits the system into two electric subsystems: one on the rectifier side, and the other inverter end. Modelling the converters within the WPGS, is of key importance and, the focus of this work.

MATERIALS AND METHODS

A. CONCEPTS AND CONFIGURATIONS

A voltage source converter (VSC) is a device that generates alternating current (AC) voltage from direct current (DC) voltage [1]. **Fig. 1** illustrates two different possible ways to integrate the VSCs into the AC system as in the WPGS. **Fig. 1(a)** represents the WPGS with either the Permanent Magnet Synchronous Generator (PMSG) or the Squirrel Cage Induction Generator (SCIG) whereas **Fig. 1(b)** represents the Doubly Fed Induction Generator (DFIG) with wound rotor [1]. Due to its robustness, low cost and flexibility to operate at variable frequency, the DFIG has been widely used. The stator supplies power straight into AC bus at the stator rotating magnetic field. On the other hand, the rotor converts 1/3 of the input power into a voltage bus which voltage level is lower than the one on the stator, at a frequency which depends on the rotor slip [1].

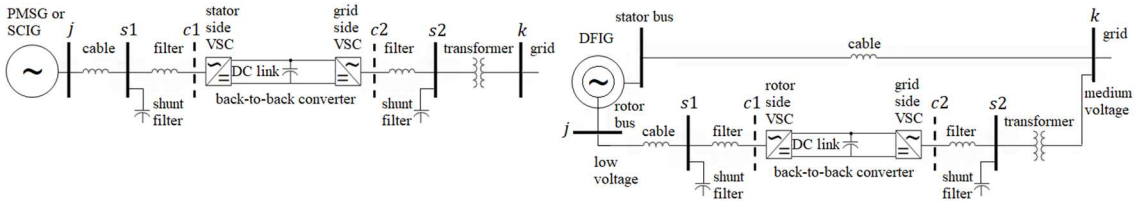

(a) (b)

Figure 1. Configuration of the generators to the power converters and grid

B. INSERTION OF THE POWER CONVERTERS INTO THE AC SYSTEM

To represent the modelling of the VSC in the back-to-back array, focus is given only to the part of the system composed of the converter and the nodes from where the connection to the grid is made, as shown in **Fig. 2**. In the block diagram, the buses *s*1 and *s*2 represent the Common Coupling Point (CCP) whereas the inner ones named *c*1 and *c*2 are placed close to the VSCs. The shunt elements, b_{s1} and b_{s2} are considered to represent filters when present in the system as much as the conductances and susceptances of the cables which connect *s*1 with *c*1, and *s*2 with *c*2.

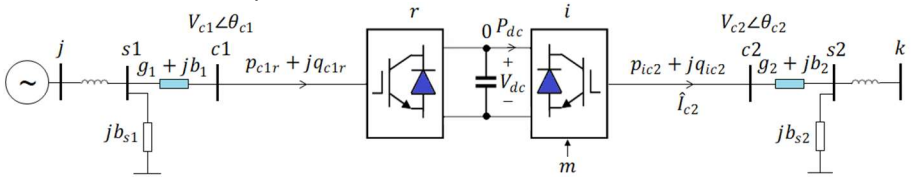

Figure 2. Highlight of the VSC converters and the interconnection with the *s*1 and *s*2 buses of the AC system, respectively the CCP1 and CCP2

In this work, the used power converter was the six step bridge with $K_C = \sqrt{6}/\pi$ [1]-[4] which is the relationship between the nodal voltage at *c*1 (V_{c1}) and DC voltage (V_{dc}). The power flow into the VSCs are computed according to Eq. (1) to (4) reference-based [2], in accordance with **Fig. 2**:

$$p_{c1r} = -g_1 V_{c1}^2 + V_{c1}V_{s1}[g_1 \cos\theta_{s1c1} - b_1 \sin\theta_{s1c1}] \quad \text{Eq. (1)}$$

$$q_{c1r} = b_1 V_{c1}^2 - V_{c1}V_{s1}[g_1 \sin\theta_{s1c1} + b_1 \cos\theta_{s1c1}] \quad \text{Eq. (2)}$$

$$p_{ic2} = g_2 V_{c2}^2 - V_{c2}V_{s2}[g_2 \cos\theta_{s2c2} - b_2 \sin\theta_{s2c2}] \quad \text{Eq. (3)}$$

$$q_{ic2} = -b_2 V_{c2}^2 + V_{c2}V_{s2}[g_2 \sin\theta_{s2c2} + b_2 \cos\theta_{s2c2}] \quad \text{Eq. (4)}$$

The notation with double subscript means the phase angle difference such as $\theta_{il} = \theta_i - \theta_l$. The power flow which comes from the CCP towards the VSCs, are:

$$p_{s1c1} = g_1 V_{s1}^2 - V_{s1}V_{c1}[g_1 \cos\theta_{s1c1} + b_1 \sin\theta_{s1c1}] \quad \text{Eq. (5)}$$

$$q_{s1c1} = -(b_1 + b_{s1})V_{s1}^2 - V_{s1}V_{c1}[g_1 \sin\theta_{s1c1} - b_1 \cos\theta_{s1c1}] \quad \text{Eq. (6)}$$

$$p_{s2c2} = g_2 V_{s2}^2 - V_{s2}V_{c2}[g_2 \cos\theta_{s2c2} + b_2 \sin\theta_{s2c2}] \quad \text{Eq. (7)}$$

$$q_{s2c2} = -(b_2 + b_{s2})V_{s2}^2 - V_{s2}V_{c2}[g_2 \sin\theta_{s2c2} - b_2 \cos\theta_{s2c2}] \quad \text{Eq. (8)}$$

When writing the power equation at buses *s*1 and *s*2 (P_{s1}, Q_{s1} and P_{s2}, Q_{s2}), there is no need to take into account the parameters of branches *s*1-*c*1 and *s*2-*c*2, and their respective shunt bus elements, to form the nodal impedance matrix. However, the power flow, as shown in Eq. (5) to (8), must be added to the injected powers into buses *s*1 and *s*2.

$$P_{s1} = G'_{s1s1}V_{s1}^2 + V_{s1}V_j\left[G'_{s1j}\cos\theta_{s1j} + B'_{s1j}\sin\theta_{s1j}\right] + p_{s1c1} \quad \text{Eq. (9)}$$

$$Q_{s1} = -B'_{s1s1}V_{s1}^2 + V_{s1}V_j\left[G'_{s1j}\sin\theta_{s1j} - B'_{s1j}\cos\theta_{s1j}\right] + q_{s1c1} \quad \text{Eq. (10)}$$

$$P_{s2} = G'_{s2s2}V_{s2}^2 + V_{s2}V_k[G'_{s2k}\cos\theta_{s2k} + B'_{s2k}\sin\theta_{s2k}] + p_{s2c2} \quad \text{Eq. (11)}$$

$$Q_{s2} = -B'_{s2s2}V_{s2}^2 + V_{s2}V_k[G'_{s2k}\sin\theta_{s2k} - B'_{s2k}\cos\theta_{s2k}] + q_{s2c2} \quad \text{Eq. (12)}$$

Eq. (9) to (12) assume that the nodal admitance matrix elements takes into account only the admitances of the branches located between *s*1 and *j* and *s*2 and *k*, respectively, being denoted by using the apostrophe (´). It means that every circuit element connected to the buses *s*1 and *s*2 and close to the power converters do not appear in the nodal admitance matrix since their role has already been taken into account at the power flow, Eq. (5) to (8) and Eq. (9) to (12).

C. POWER CONVERTERS REPRESENTED AS LOADS AT *c*1 AND *c*2

The proposed model assumes that, from the rectifier side, the active power is the same as the one at the DC link whereas the reactive one is zero. The inverter behaves as a voltage source, which active power to be delivered into the AC system is the same as in the DC link, minus the losses. Then, the system is modelled as if the DC link could supply apparent power to the grid. Inspired by reference [4]-[5], as shown in **Fig. 3**, the active load is placed at the rectifier's terminals.

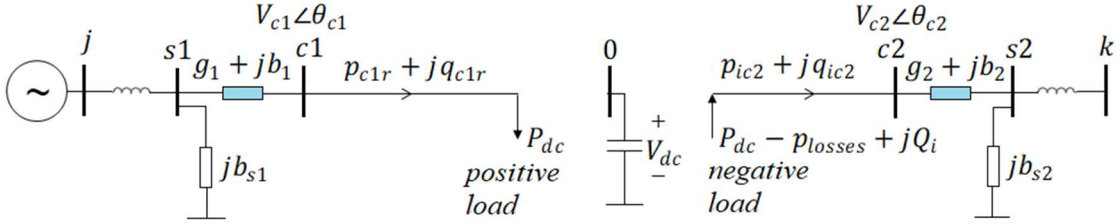

Figure 3. Rectifier and inverter replaced by loads at buses *c*1 and *c*2

At the inverter's output, the active power is the DC power minus the losses in the VSCs, and the reactive power Q_i, is a value to be specified by the user. The power balance must then be written according to Eq. (13) to (16) which represent a mismatch of the powers at buses *c*1 and *c*2. The term 'specified' is abreviated by *sp*.

$$\Delta P_{c1} = P_{c1}^{sp} - P_{c1} = P_{dc} - p_{c1r} = 0 \quad \text{Eq. (13)}$$

$$\Delta Q_{c1} = Q_{c1}^{sp} - Q_{c1} = 0 - q_{c1r} = 0 \quad \text{Eq. (14)}$$

$$\Delta P_{c2} = P_{c2}^{sp} - P_{c2} = P_{dc} - p_{losses} - p_{ic2} = 0 \quad \text{Eq. (15)}$$

$$\Delta Q_{c2} = Q_{c2}^{sp} - Q_{c2} = Q_i^{sp} - q_{ic2} = 0 \quad \text{Eq. (16)}$$

D. POWER LOSSES IN VSCs

The internal losses of the VSC with electronic component such as IGBTs are formed by three parts: *i*) losses which are non-dependant on its operation, p_{off}; *ii*) switching losses, p_{sw}; and *iii*) Ohm's losses, p_{cond}. Usually, the losses associated with the VSCs range from 1% to 2% of its rated value [4]. In this work, the quadratic model is considered, which coefficients are defined for each case under study [5].

$$p_{losses} = a + bI_{c2} + cI_{c2}^2 \quad \text{Eq. (17)}$$

The output current, in per unit (p.u), is computed as follows [5]:

$$I_{c2} = \sqrt{p_{ic2}^2 + q_{ic2}^2}/V_{c2} \quad \text{Eq. (18)}$$

E. JACOBIAN MATRIX STRUCTURE WITH VSCs

In the proposed model, the back-to-back VSCs implies in the inclusion of two lines and columns in each of the submatrix which forms the Jacobian matrix. Naturally, it demands the increase of 4 elements mismatches into ΔF vector, as defined from Eq. (13) to (16), and 4 corrections in ΔX vector, that are $\Delta\theta_{c1}$, $\Delta\theta_{c2}$, ΔV_{c1}e ΔV_{c2}, to the iteration equations of the Newton load flow [2].

$$\Delta F = \begin{bmatrix} H & N \\ M & L \end{bmatrix} \Delta X \quad \text{Eq. (19)}$$

The submatrices of the Jacobian matrix are then written in accordance with the lines and columns numbers *j*, *s*1, *s*2, *k*, *c*1 e *c*2, of the systems as illustrated in **Fig. 2** and **Fig.3**. However, due the lack of space, will not be presented here. The VSCs' losses depend on unknown variables of the load flow then, the differentiation of P_{c2} in matrix H and N involves the differentiation of p_{losses} and p_{ic2}, as shown in Eq. (15), specifically the elements $\partial P_{c2}/\partial\theta_{s2}$, $\partial P_{c2}/\partial\theta_{c2}$, $\partial P_{c2}/\partial V_{s2}$ and $\partial P_{c2}/\partial V_{c2}$.

The iterations of the Newton's method require an update of the Jacobian matrix elements at each step. Should there be a system with nb buses and nc VSCs, the Jacobian matrix will be enlarged by $2nc$ lines and $2nc$ columns, and each submatrix, $nb + nc$ lines and the same number of columns. The mismatches and correction vectors will be enlarged in the same proportion as the Jacobian matrix.

F. POWER AND SYSTEM BUSES RATING

The available active power at the shaft of wind turbine varies according to the wind speed. Then, it is convenient to use the wind turbine rotating speed (n) as the input and, from this information, compute the power P_w. The power as a function of the speed, n , is given according to Eq. (20).

$$P_w = P_{w,max} - (n_{max} - n)\frac{P_{w,max} - P_{w,min}}{n_{max} - n_{min}} \quad \text{Eq. (20)}$$

RESULTS AND DISCUSSION

This section presents the computation of the load flow problem of a WPGS inspired by the Fortim Wind Generation Compound located in the northeast of Brazil [3]. The applicability of the proposed modelling of the VSCs within the system, by using Newton algorithm, is demonstrated by the simulation results.

A. ELECTRICAL SYSTEMS

Two electrical systems were tested together with a modification of the DFIG configuration which suggests the use of a '*dummy transformer*' (DT).

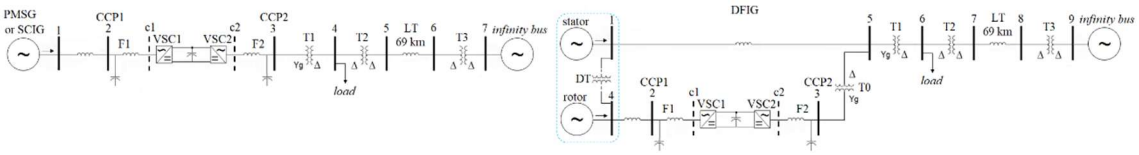

(a) (b)

Figure 4. Test-systems: (a) with PMSG or SCIG; (b) DFIG

The system in **Fig. 4(b)** is the most similar to Fortim's, except for the DT. In the system as shown in **Fig. 4(a)**, the bus number 7 is the *infinity bus*, which is the grid bus where voltage and frequency are known and kept unchanged. For the other system as shown in **Fig. 4(b)**, this bus is the one numbered 9. The electrical parameters are displayed in **Tab. 1** with the data given in per unit (p.u) taken 100 MVA and the node voltages as the base values. The shunt elements represent the capacitive admittances of the system's filters, which values are 0.0003 p.u, corresponding at 30 kvar in respective voltage. On buses 4 and 6, at 34.5 kV, there is a load equal to 1 MW and 0.75 Mvar.

Table 1. Electrical parameters in p.u of **Fig. 4** systems

Fig. 4(a)	branch	1-2	2-*c*1	*c*2-3	T1	T2	5-6	T3	–	–
	r	0.01	0.5	0.5	0.3	0.4	0.05	0.02	–	–
	x	0.02	0.5	0.5	0.8	0.8	0.15	0.08	–	–
Fig. 4(b)	branch	4-2	2-*c*1	*c*2-3	1-5	T0	T1	T2	7-8	T3
	r	0.01	5.0	5.0	0.01	1.5	0.3	0.4	0.05	0.02
	x	0.02	5.0	5.0	0.02	4.0	0.8	0.8	0.15	0.08

The Fortim compound has 123MW of installed power capability. However, only 9 generators supply power to the Jandaia 12/34.5kV substation [3], represented by the transformer T1 in **Fig. 4(a)** and **Fig. 4(b)**. In this simulation, only the 3MW wind turbine was considered. Such power was assumed to be the one supplied by the wind turbine to the generator at bus 1 in **Fig. 4(a)**. In the single-phase diagram shown in **Fig. 4(b)**, power is delivered to the wound induction generator which is represented by the stator and rotor: buses 1 and 4. If the DT is added, the impedance was set to 1+*j* p.u between buses 1 and 4, ratio 12/0.69kV. Because of this, both buses can be assigned to be the PV type, avoiding the need to create two slack buses in the system. By using a 1:100 gear ratio, the generator speed ranges from 920 – 1,560rpm. Simulation was carried out by considering an induction generator running at 1,400rpm, which corresponds to an active power P_w = 3.106MW. The voltage was setup to 102% at bus 1 and 100% at the *infinity bus*, which is the bus number 7 in **Fig. 4(a)** and bus number 9 in **Fig. 4(b)**. Since the inverter operates with unity power factor, the reactive power, Q_i in **Fig. 3**, was set up to zero, Q_i^{sp} = 0. The mismatches tolerance to the load flow was setup to 10^{-6}. To evaluate losses in the converters, we arbitrate 10^{-4}, $30\text{x}10^{-4}$ and $2\text{x}10^{-4}$, for a, b and c, respectively. The load flow for the system shown in **Fig. 4(a)** converged after 11 iterations and, for the systems shown in **Fig. 4(b)** without and with DT, converged after 91 and 88 iterations, respectively. The results obtained from the load flow computation is presented in **Tab. 2**, where the specified values are shown in bold character and the buses rated voltages in the 'kV' column.

The active power delivered into the grid is shown in **Tab. 3**. The negative signal means that the bus (*i.e.*, Brazilian Integrated System represented by the Russas 230 kV bus [3]) is receiving the power produced by the wind turbine, minus 1MW due to load at buses 4 and 6 and the losses. The DC link powers are shown and the losses in the system's components, including the VSCs' losses.

Table 2. Node voltages with modules in p.u and angles in degree at the AC systems

Bus	**Fig. 4(a)**		**Fig. 4(b)** without DT		**Fig. 4(b)** with DT	
	kV	Results	kV	Results	kV	Results
1	12	slack) **1.0200∠0⁰**	12	PV) **1.0200**∠2.5236⁰	12	PV) **1.0200**∠2.4060⁰
2	12	1.0197∠−0.0404⁰	0.69	0.9999∠−0.0144⁰	0.69	0.9999∠3.4377⁰
3	12	1.0092∠2.7965⁰	0.69	1.0327∠4.6424⁰	0.69	1.0327∠4.5262⁰
4	34.5	1.0005∠1.4133⁰	0.69	slack) **1.0000∠0⁰**	0.69	PV) **1.0000**∠3.4521⁰
5	230	0.9994∠0.2982⁰	12	1.0197∠2.5042⁰	12	1.0197∠2.3879⁰
6	230	0.9997∠0.1015⁰	34.5	1.0065∠1.2445⁰	34.5	1.0065∠1.1776⁰
7	230	slack) **1.0000∠0⁰**	230	1.0007∠0.2736⁰	230	1.0008∠0.2594⁰
8	-	-	230	1.0002∠ 0.0945⁰	230	1.0002∠ 0.0897⁰
9	-	-	230	slack) **1.0000∠0⁰**	230	slack) **1.0000∠0⁰**

Table 3. Active power, DC link power and losses

System	Active power injection (MW)			P_{dc}	Total losses
	Bus 1	Bus 4	*Infinity bus*	(MW)	(kW)
Fig. 4(a)	3.1543	-	−1.9914	3.1055	162.8330
Fig. 4(b) without DT	2.0703	1.0955	−1.9873	1.0352	178.4560
Fig. 4(b) with DT	2.0703	1.0352	−1.8934	1.0352	212.0470

The losses in VSCs are 19.059 kW (**Fig. 4(a)**) and 12.844 kW (**Fig. 4(b)** with or without DT). For the system with DT, the losses only in this equipment are 37.001 kW. The results shown in **Tab. 4** are voltages and currents associated to the power converters, including the DC link voltage and converter's modulation index. The analysed configurations result in overmodulated converters.

Table 4. Results associated with the power converters and DC link voltage

Quantities	**Fig. 4(a)**	**Fig. 4(b)** without DT	**Fig. 4(b)** with DT
V_{c1} (p.u)	1.0041	0.9435	0.9435
I_{c1} (p.u)	0.0309	0.0110	0.0110
V_{c2} (p.u)	1.0241	1.0783	1.0783
I_{c2} (p.u)	0.0301	0.0095	0.0095
modulation index (adim.)	1.0200	1.1442	1.1442
V_{dc}(kV)	15.4530	0.8340	0.8340

The scheme in **Fig. 4(a)** imposes high voltage on the DC link. In **Fig. 4(b)**, the results without and with DT in **Tab. 4** are identical, with the difference being noted in the losses (as in **Tab. 3**), allowing the modeling of losses in the generator.

CONCLUSION

This work presented the modelling of the steady state analysis of a back-to-back VSCs existing in WPGS, by the though the load flow implementation. The new algorithm is based on the modification of the classical load flow method by inserting new derivatives in the Jacobian matrix structure. The results presentation of the proposed method was carried out by using real parameters of Fortim's WPGS located at Ceara state. The algorithm and the results obtained contribute to improving the operator's decisions and planners of Power System Control Centers.

ACKNOWLEDGMENT

This work is a product of the P&D-00394-1903/2019 project, with financial support from Furnas and managed by FUNAPE, to which we are grateful.

REFERENCES

[1] Abad, G. et al. "Back-to- back power electronic converter" in *Doubly Fed Induction Machine Modeling and Control for Wind Energy Generation*. New Jersey: Willey, 2011, chap 2, pp. 87–154.

[2] Monticelli, A. *Fluxo de carga em redes de energia elétrica*. São Paulo: Blücher, 1983, pp.1-164.

[3] Projeto Fortim: Energia Eólica, "Anexo IV: Especificações técnicas dos aerogeradores e descritivo do SCADA", Eletrobras, Furnas, Tech. Rep. CT.EDV.ENG.006.2018, 2018.

[4] Liang, H. et al. "*Study of Power Flow Algorithm of AC/DC Distribution System including VSC-MTDC*", *Energies, Open Access,* v8, pp. 8391-8405, Aug. 2015.

[5] Khan, M. et al. "*A Load Flow Analysis for AC/DC Hybrid Distribution Network Incorporated with Distributed Energy Resources for Different Grid Scenarios*", *Energies,* v11, 367, 1–15, Feb.2018.